ORIGINAL ARTICLE

DOI: 10.4274/eamr.galenos.2023.72677
Eur Arch Med Res 2023;39(4):254-261

Evaluation of Dynamic Contrast Breast Magnetic Resonance Imaging Findings in Molecular Subtypses of Breast Cancer According to Birads Descriptions

Nigar Erkoç[1], Ayşegül Akdoğan Gemici[2], Ercan İnci[2]

[1]University of Health Sciences Turkey, Bağcılar Training and Research Hospital, Clinic of Radiology, İstanbul, Turkey
[2]University of Health Sciences Turkey, Bakırköy Dr. Sadi Konuk Training and Research Hospital, Clinic of Radiology, İstanbul, Turkey

Abstract

Objective: Our aim is to reveal the correlation between the molecular subtypes of breast cancer (BC) and contrast-enhanced breast magnetic resonance imaging (MRI) findings and to determine the possible molecular subtype and prognosis of the breast mass before the operation according to the MRI findings. In this way, it is aimed to ensure that contrast-enhanced breast MRI guides diagnosis and treatment.

Methods: This study was conducted retrospectively between June 2015 and October 2020 including 265 patients who underwent dynamic contrast-enhanced breast MRI in our hospital and whose pathology results were consistent with invasive breast carcinoma. As a result of histopathological studies, patients were divided into molecular subtypes according to hormone receptor status (estrogen, progesterone, human epidermal growth factor receptor-2), and Ki-67 level, and MRI findings were evaluated for these subtypes according to the "Breast Imaging Reporting and Data System" updated in 2014 by the American College of Radiology.

Results: A total of 265 cases of invasive BC were included. In these cases, the most common subtype was luminal A in 93 cases (35%), 79 luminal B tumor cases (29.8%), 51 triple-negative tumors (19.3%), and 42 HER2 tumor cases (6.7%). There was a statistically significant difference between molecular subtypes in terms of MRI findings and lesion presentation ($p<0.0001$). In addition, statistical analyses showed that there was a significant difference between the subgroups of mass shape and contour. In our study, no significant difference was found between the contrast enhancement pattern and contrast enhancement kinetic curves between molecular subtypes.

Conclusion: There is a correlation between molecular subtypes and some MRI findings, and molecular subtypes can be determined early before the operation and prognostic markers can be revealed earlier.

Keywords: Breast cancer, hormone receptors, breast magnetic resonance imaging

INTRODUCTION

Invasive breast cancer (BC) is the most common type of cancer in the female population and is the second leading cause of death after lung cancer. BC accounts for approximately 30% of all cancers diagnosed in women and approximately 17-18% of cancer-related deaths (1).

Magnetic resonance imagining (MRI) is a non-invasive imaging technique that provides information about the location and prevalence of malignancy as well as evaluates tissue characteristics, which can aid in monitoring and predicting treatment response and guide patient management. However, some authors went beyond diagnostic characteristics and investigated the efficacy of MRI in the response to chemotherapy. We further investigated this subject and showed the sensitivity of MRI by monitoring the chemotherapy response of molecular subtypes (2). MRI provides functional features not only with morphological parameters but also through kinetic curves

Address for Correspondence: Nigar Erkoç, University of Health Sciences Turkey, Bağcılar Training and Research Hospital, Clinic of Radiology, İstanbul, Turkey
E-mail: ngrgltkn@gmail.com **ORCID ID:** orcid.org/0000-0002-2162-9284

Received: 13.05.2023
Accepted: 06.07.2023

Cite this article as: Erkoç N, Akdoğan Gemici A, İnci E. Evaluation of Dynamic Contrast Breast Magnetic Resonance Imaging Findings in Molecular Subtypses of Breast Cancer According to Birads Descriptions. Eur Arch Med Res 2023;39(4):254-261

related to tumor biology (3). Some publications have stated that dynamic contrast-enhanced breast MRI parameters are correlated with tumor vascularity and may display differences between histopathological types (4-9).

Invasive BC is often classified primarily by its histological appearance. Today, some subtypes have been defined, including their molecular properties. These subtypes were first classified in 2,000 on the basis of gene expression studies, which are still valid today (8). In this classification, invasive cancers are identified as luminal A, luminal B, human epidermal growth factor receptor-2 (HER2), and triple-negative (TN) BC according to their biological markers. These different molecular subtypes display differences in disease prognosis, treatment approach, and post-treatment follow-up according to estrogen receptor (ER), progesterone receptor (PR), HER-2 positivity, and nuclear Ki-67 expression. The luminal- A subtype (ER-positive, HER2 negative, or PR weak or strong positive) responds to hormone therapy and usually has an excellent prognosis. Luminal B (can be ER positive, HER2 negative or positive, PR positive or negative) exhibits a worse prognosis than Luminal A but tends to be better than the HER2 (+) subtype in general.

The HER2 (+) (HER2 positive, ER and PR negative) subtype, on the other hand, is more aggressive but can be treated with monoclonal antibodies targeting the erbB-2 membrane receptor. TN, BC (ER, PR, and HER2 negative) is the most aggressive subtype and usually responds to chemotherapy (2). Therefore, early detection of BC subtypes can help start treatment and determine prognosis without wasting time.

This study aimed to retrospectively show the correlation of dynamic contrast-enhanced MRI-derived parameters between BC molecular subtypes according to the Breast Imaging Reporting and Data System (BI-RADS).

METHODS

Data of 265 patients who underwent preoperative contrast-enhanced breast MRI between June 2015 and October 2020 and were diagnosed with invasive BC by biopsy and whose subtypes were determined were retrospectively screened from the hospital system. Ethics committee approval was obtained for this study from the Ethics Committee of University of Health Sciences Turkey, Bakırköy Dr. Sadi Konuk Training and Research Hospital with decision number 2020/538 and dated 21.12.2020.

Patients were compared in terms of demographic characteristics and radiological and histological/histopathological findings. Immunohistochemical data in pathology reports obtained with the biopsy of BC molecular subtypes were classified into 4 subgroups according to ER and PR receptor status, HER2, and Ki-67 levels. Molecular subtypes of BC according to the latest St. Gallen Internotional Expert Consensus (2013) immunohistochemical findings were categorized into 4 subtypes: luminal A [ER (+) or PR (+) and Ki-67 ≤20%], luminal B [ER (+) or PR (+) and Ki-67 ≥20% and HER-2 (+) and ER (+) and Ki-67 insignificant], HER-2 rich (ER and PR positive\negative and HER-2 positive), and (TN) BC basal-like cases [ER (-), PR (-) HER-2 (-) (Table 1)].

Inclusion criteria were patients with preoperative contrast-enhanced breast MRI findings belonging to patients who were histopathologically (tru-cut, excisional, or incisional biopsy) diagnosed with invasive BC and whose molecular subtypes were determined were included in the study.

Exclusion criteria were as follows: patients with insufficient MRI results for diagnosis, receiving neoadjuvant chemotherapy prior to MRI, operated for BC and receiving chemotherapy treatment, recurrence of cancer, patients with breast implants, and patients with unknown tumor histology (Figure 1).

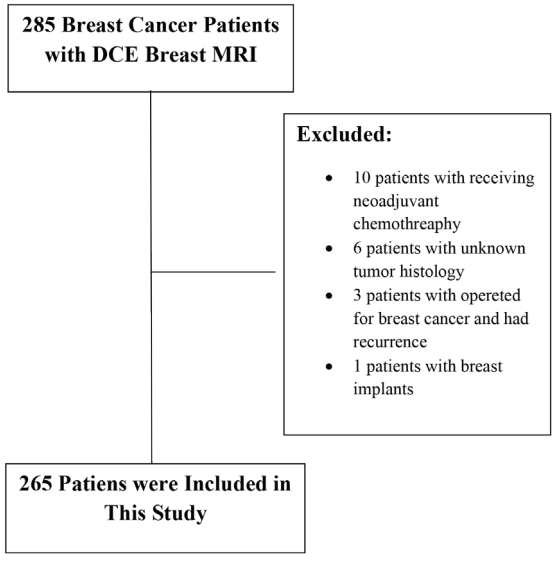

Figure 1. Flow chart of study population

Table 1. Biomarker profile of breast cancer molecular subtypes

Molecular subtype	Immunohistochemical biomarker profile
Luminal A	ER+ and/or PR+, HER2 (-) and low Ki67 (<20%)
Luminal B	ER+ and/or PR+, HER2 (+) (luminal HER2 group)- ER+ and/or PR+, HER2 (-) and high Ki67 (>20%)
HER2(+)	ER-, PR- and HER2 (+)
Triple negative (Basal-Like)	ER-, PR-, HER2-

Dynamic Contrast-Enhanced Magnetic Resonance Imaging

MRI examinations were performed in the prone position using a breast coil with the 3.0 Tesla MRI (Siemens, Verio Healthcare, Erlangen, Germany) device in our clinic. Fat-suppressed axial SE T2-weighted, pre-contrast axial T1-weighted, contrast-enhanced dynamic fat-pressed axial T1-weighted, and post-contrast fat-pressed axial and sagittal T1-weighted sequences were obtained for all patients. In dynamic examinations, following the acquisition of non-contrast-enhanced images, contrast-enhanced images were obtained with IV administration of 0.1-0.2 mmol/kg gadolinium-containing contrast agent at a rate of 2 mL/s based on the weight of the patient. Six phasic serial images were obtained for each section at 30-s intervals for dynamic contrast-enhanced T1-weighted sequences.

Pre-contrast images were extracted from the corresponding post-contrast images using a subtraction program through special software on the MR device console over the dynamic images obtained.

Lesions were grouped and examined using the latest BI-RADS according to dynamic contrast-enhanced MRI findings. Following this, they were morphologically categorized as focus, mass, non-mass enhancement, and mass/non-mass enhancement groups. Mass lesions were examined according to shape, margin, and internal enhancement patterns, whereas non-mass enhanced lesions were examined according to distribution and internal enhancement patterns.

The dynamic contrast enhancement curves of the cases were examined using the Syngo Via device. Dynamic curves were created according to the peak contrast enhancement values. Dynamic curves were classified as Types 1, 2, 3.

Statistical Analysis

Descriptive data were expressed as mean, standard deviation, median, highest and lowest values, frequency, and ratio. The distribution of variables was tested using the Kolmogorov-Smirnov test. Quantitative independent data were analysed using the Mann-Whitney U test. Dependent quantitative data were analyzed using the Wilcoxon test.

The chi-square test was used for the analysis of qualitative independent data, whereas Fisher's Exact test was used when the chi-square test requirements were not met. Intraclass correlation analysis was performed to analyse the correlations. Data analysis was performed using IBM SPSS Statistics for Windows (Version 27.0) program.

RESULTS

General Characteristics of the Patients

The study was conducted with 265 patients diagnosed with BC between June 2015 and October 2020. The mean age of the patients was 50.41±81.02 years (Tables 1 and 2).

According to the pathological biopsy results of 265 cases diagnosed with BC, 248 had IDC, 12 had ILC, and 5 had IDC and ILC combined (Table 3).

The most common molecular subtypes were luminal A (35%) and luminal B (29.8%), followed by TNBC (19.3%) and HER2+ (15.8%).

Radiological and Pathological Findings

Of the cases included in the study, 170 had ER, 137 had PR, and 71 had HER2 positives (+). Considering these findings, the classification of Ki-67 percentages and molecular subtypes revealed that 93 patients had luminal A, 79 patients had luminal B, 42 patients had HER2 (+), and 51 patients had TNBC subtypes (Table 4).

Axillary lymph node involvement did not differ between BC subtypes. Among the patients with lymph node involvement (+), luminal B was observed at a rate of 33.59%, luminal A at 28.24%, HER2 (+) tumors at 21.37%, and TNBC at 16.79% (Table 5).

According to the MRI findings, evaluation of mass presentation as mass, non-mass enhancement, and mass/non-mass enhancement revealed a statistically significant difference between the molecular subtypes ($p<0.0001$). The non-massive enhancement rate alone and the association of mass/non-mass enhancement in the HER2 (+) group were found to be higher than those in the other groups (Figures 2 and 3)

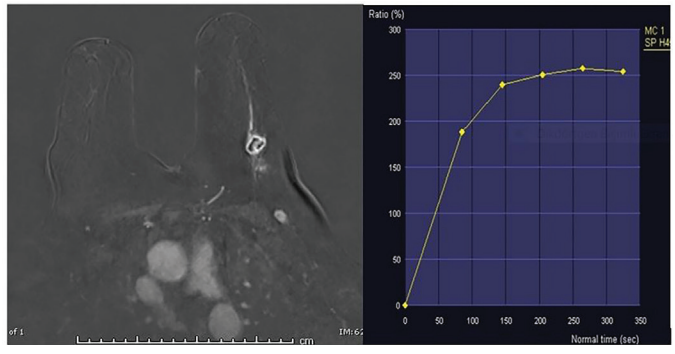

Figure 2. Triple negative breast cancer in 60- year-old women-Substracted T1-weighted contrast-enhanced image shows oval shape mass with circumscribed margins and rim enhancement. The lesion shows a Type 2 contrast enhancement pattern

Statistical analyses revealed a significant difference between molecular subtypes in terms of mass shape (p<0.001). TNBC, in particular, often displayed more regular shapes (oval, round). Luminal A lesions mostly displayed an irregular shape. A comparison of mass margins revealed a significant difference between the molecular subtypes (p<0.001). The luminal A and luminal B subtypes displayed irregular and spiculated margins, whereas the TNBC group displayed significantly sharper margins. There was no significant difference in contrast enhancement patterns between the subtypes (p=0.23). In addition, no significant difference was observed in enhancement kinetic

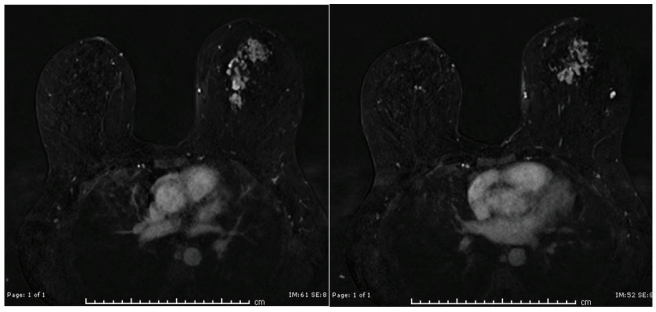

Figure 3. HER2 (+) breast cancer in 53 year-old women-substracted T1 weighted contrast enhanced image shows heterogenous non mass enhancement and regional distribution dynamic series

Table 2. Demographic and molecular findings of the patients

		Min-max	Median	Mean + SD/n-%	
Age		27-81	48.0	50.41±12.02	
Pathological size		3-80	25.0	25.02±11.60	
MRI mass size		6.0-113	30.0	31.75±16.56	
ER	(-)			95	35.8%
	(+)			170	64.2%
PR	(-)			128	48.3%
	(+)			137	51.7%
HER2	(-)			194	73.2%
	(+)			71	26.8%

Min: Minimum, Max: Maximum, SD: Standard deviation

Table 3. Distribution of histopathological findings of molecular subtypes

		Luminal A n=93		Luminal B n=79		HER2 pozitive n=42		Triple N. n=51	
		n	%	n	%	n	%	n	%
Histological type	IDC	79	84.9%	77	97.5%	41	97.6%	51	100%
	ILD	14	15.1%	2	2.5%	1	2.4%	0	0.0%
Histological grade	Low	17	18.3%	3	3.8%	0	0.0%	1	2.0%
	Intermediate	52	55.9%	51	64.6%	20	47.6%	17	33.3%
	High	12	12.9%	12	15.2%	8	19.0%	20	39.2%

Table 4. Distribution of pathological and MRI findings of molecular subtypes

	Luminal A n=93		Luminal B n=79		HER 2 pozitive n=42		Triple N. n=51	
	Mean ± SD/n-%		Mean ± SD /n-%		Mean ± SD /n-%		Mean ± SD /n-%	
Age	56.6±12.0		48.3±13.3		51.7±10.1		48.7±10.9	
Pathological size	22.8±10.5		26.7±11.0		31.4±18.0		25.3±10.8	
MRI mass size	25.6±13.9		35.1±17.4		37.6±17.7		33.0±15.6	
Kİ 67	8.6±5.9		39.1±21.9		36.0±21.9		47.5±27.8	
Premenopausal	48	51.6%	32	40.5%	23	54.8%	21	41.2%
Postmenapausal	45	48.4%	47	59.5%	19	45.2%	30	58.8%

SD: Standard deviation

Table 5. Comparison of axillary lymph node metastasis of molecular subtypes

		Luminal A n=93		Luminal B n=79		HER2 pozitif n=42		Triple N. n=51	
		n	%	n	%	n	%	n	%
Axillary lymph node metastasis	No	56	60.2%	35	44.3%	14	33.3%	29	56.9%
	Yes	37	39.8%	44	55.7%	28	66.7%	22	43.1%

curves between molecular subtypes, whereas plateau and wash out occurred at a higher rate in all subtypes.

Among the molecular subtypes of BC, the presence of accompanying foci also showed a minimally significant difference between the groups (p=0.008).

In cases with non-mass enhancement, no significant difference was noted between the subtypes in terms of distribution or enhancement pattern. However, the segmental and diffuse non-mass enhancement rate was significantly higher (p<0.05) in HER2 (+) cases than in HER2 (-) cases. The rates of focal, linear,

Table 6. Comparison of molecular subtypes according to BI-RADS features

		Group				
		Luminal A	Luminal B	HER2	Triple negative	P
		n (%)	n (%)	n (%)	n (%)	n (%)
Metastasis	Unifocal	67 (33.67)	58 (29.15)	28 (14.07)	46 (23.12)	0.202
	Multifocal	18 (39.13)	14 (30.43)	10 (21.74)	4 (8.7)	
	Multicentric	7 (36.84)	7 (36.84)	4 (21.05)	1 (5.26)	
Axillary lymph node involvement	No	56 (41.79)	35 (26.12)	14 (10.45)	29 (21.64)	0.015
	Yes	37 (28.24)	44 (33.59)	28 (21.37)	22 (16.79)	
Focal	No	81 (39.71)	55 (26.96)	27 (13.24)	41 (20.1)	**0.008**
	Yes	12 (19.67)	24 (39.34)	15 (24.59)	10 (16.39)	
Presentation	Focal	0 (0)	0 (0)	0 (0)	0 (0)	**0.0001**
	Mass	71 (37.97)	64 (34.22)	16 (8.56)	36 (19.25)	
	Non-mass contrast enhancement	0 (0)	2 (40)	3 (60)	0 (0)	
	Mass + non-mass enhancement	22 (30.14)	13 (17.81)	23 (31.51)	15 (20.55)	
Mass shape	Oval	3 (14.29)	5 (23.81)	0 (0)	13 (61.9)	**0.0001**
	Round	6 (17.14)	12 (34.29)	3 (8.57)	14 (40)	
	Irregular	84 (41.18)	60 (29.41)	36 (17.65)	24 (11.76)	
Mass margin	Sharp	4 (12.12)	4 (12.12)	2 (6.06)	23 (69.7)	**0.0001**
	Irregular	45 (30.82)	53 (36.3)	23(15.75)	25 (17.12)	
	Spiculated	44 (54.32)	20 (24.69)	14 (17.28)	3 (3.7)	
Enhancement pattern	Homogeneous	6 (66.67)	1 (11.11)	1 (11.11)	1 (11.11)	0.230*
	Heterogeneous	63 (36)	57 (32.57)	26 (14.86)	29 (16.57)	
	Circular enhancement	24 (31.58)	19 (25)	12 (15.79)	21 (27.63)	
	Contrast-enhanced/non-enhanced septations	0 (0)	0 (0)	0 (0)	0 (0)	
Non-mass contrast-enhancement distribution	Focal	1 (9.09)	5 (45.45)	4 (36.36)	1 (9.09)	0.333*
	Linear	4 (33.33)	2 (16.67)	3 (25)	3 (25)	
	Segmental	15 (34.09)	6 (13.64)	13 (29.55)	10 (22.73)	
	Regional	2 (40)	1 (20)	1 (20)	1 (20)	
	Multi-regional	0 (0)	0 (0)	1(50)	1(50)	
	Diffuse	0 (0)	2 (33.33)	4 (66.67)	0 (0)	
Non-mass contrast enhancement pattern	Homogeneous	0 (0)	0 (0)	1 (100)	0 (0)	0.8268*
	Heterogeneous	7 (21.88)	5 (15.63)	11 (34.38)	9 (28.13)	
	Cobblestone/cluster	12 (33.33)	8 (22.22)	11 (30.56)	5 (13.89)	
	Clustered rings	3 (27.27)	3 (27.27)	3 (27.27)	2 (18.18)	
Kinetic curve pattern	Type I	6 (50%)	0	0	6 (50%)	
	Type II	49 (34.5%)	48 (33.8%)	21 (14.8%)	24 (16.9%)	
	Type III	38 (34.3%)	31 (27.9%)	21 (18.9%)	21 (18.9%)	

*Fisher Freeman Halton test
Chi-square analysis

regional, and multiple regional non-mass enhancement did not differ significantly (p>0.05) between in the HER2 (-) and HER2 (+) groups (Table 6).

DISCUSSION

In this study, we aimed to investigate the relationship between different molecular subtypes of breast carcinoma and MRI findings according to the BI-RADS classification. In our study, a comparison of mass presentation patterns between molecular subtypes revealed that non-mass enhancement and coexistence of mass and non-mass enhancement had a significantly higher rate in the HER2 (+) subtype (p<0.0001). In addition, the comparison of HER2 (+) and HER2 (-) cases revealed that only mass and presentation were significantly lower (p<0.05). Similar to our study, Navarro Vilar et al. (10) found a significantly higher distribution of non-mass enhancement in the HER2 (+) subtype (p=0.003). In the study by Süha Öztürk et al. (12), no significant difference was found with respect to subtypes between mass and non-mass enhancement patterns and no significant difference between subtypes in the distribution and patterns of non-mass enhancement.

A significant difference was observed in the comparison of mass shapes by subtype among the cases presenting with mass and mass/non-mass enhancement (p<0.0001). In our study, although the oval shape was significantly higher in TNBC cases compared with other subtypes, the irregularly circumscribed mass was found to be significantly higher in the luminal A subtype. Again, significant differences were observed among the mass margins of the 4 subtypes (p<0.0001). While circumscribed margins were more common in TNBC cases (69.7%), spiculated margins were significantly more common in luminal cases (54.32%). The study by Navarro Vilar et al. (10) reported similar results to our study. In this study, TNBC cases were frequently in the form of a mass and presented with a round shape and circumscribed margins. Luminal A cases mostly exhibited mass enhancement with irregular shape and spiculated margins (10). In their review, Ab Mumin et al. (11) compared MRI findings of molecular subtypes and reported that oval/round shape (n=6) was more frequent in TNBC cases, whereas only one study reported lobule shape (n=1). Again, in the same review, mass margins were mostly circumscribed in TNBC cases.

In our study, HER2 (+) cases mostly presented with mass + non-mass enhancement; however, HER2 (+) cases with mass enhancement presented with highly irregular mass shapes and often irregular and spiculated mass margins. When compared with similar studies, our results show significant consistency in terms of mass margin but differ in terms of mass shape. For example, Youk et al. (13) and Navarro Vilar et al. (10) yielded similar results in their studies, reporting mostly round and oval shapes and spiculated margins in the HER 2 (+) subtype. In the review of Ab Mumin et al. (11), mass shape was evaluated in 6 of 19 HER2 (+) studies, in which 4 studies reported frequently irregular shapes and 2 studies reported round shapes. Additionally, there were 4 studies reporting spiculated/irregular margins and 2 studies reporting circumscribed margins in the same review, similar to our study.

In our study, most luminal B cases (64/79) presented with mass lesions often with irregular and irregular/spiculated contours. In another study, mass presentation was mostly observed in the luminal B subtype, similar to this study, often displaying round/irregular shapes and spiculated margins (10). Additionally, although the same study reported similar morphological characteristics between luminal B, luminal A, and HER2 (+) tumors, the number of luminal B and HER2 (+) tumors in the study was significantly lower compared with our study (10). Although 19 of our luminal B subtype cases were HER2 (+) and 60 were HER2 (-), no morphological comparison was performed between the cases in this study.

Although we found no significant difference in mass enhancement patterns among molecular subtypes (p=0.23), our results are consistent with the results of available studies. Heterogeneous enhancement was observed at a rate of 56.9% and rim enhancement at a rate of 41.2% among (TN) BC cases included in our study. Heterogeneous enhancement was more predominant in luminal A, luminal B, and HER2 (+) at 59.5%. In a similar study by Navarro Vilar et al. (10), mass enhancement patterns differed significantly between subtypes (p=0.045), with rim enhancement (68.7%) and heterogeneous enhancement patterns (31%) being significantly higher in (TN) BC cases. In addition, no homogeneous contrast enhancement was detected among (TN) BC cases in this study. In the same study, rim enhancement was observed in 33%, and septation enhancement was observed in 30% of luminal A cases. In a similar study by Algazzar et al. (14), a comparison of radiological findings according to molecular subtypes and HER2 receptor expression revealed significantly higher rim enhancement in (TN) BC cases 66.7%. In the same study, heterogeneous enhancement was observed at a rate of 70.6% in luminal A cases, 70% in luminal B cases, and 85% in HER2 (+) cases.

In the study by Uematsu et al. (15) comparing (TN) BC cases with ER (+)\PR (+)\HER2 (-) cases, ER (+)\PR (+)\HER2 (-) cases displayed irregular\oval shape, irregular margins, and heterogeneous

enhancement. Similar MRI findings were found in the study by Youk et al. (13).

Dynamic contrast-enhanced MRI provides information not only on mass morphology but also tissue perfusion and enhancement kinetics. It helps display strong and early enhancement and wash out in the late phases, especially in lesions with high vascularization, such as BC (16). In our study, no significant difference was observed in the kinetic contrast enhancement curves between the subtypes, whereas wash out and plateau curves were frequently observed in the late phases.

A meta-analysis by Kazama et al. (17) reported that the wash out curve was very common in BC cases but was insufficient to identify subtypes. Again, in the same meta-analysis, it was emphasized that the type 3 curve was observed at a higher rate in HER2 (+) cases than in HER2 ( ) cases, with no significant difference in ER (+) and ER ( ) cases. In a similar study, Navarro Vilar et al. (10) found no significant difference between dynamic contrast enhancement curves and subtypes, frequently observing plateau and wash out curves.

In our study, only non-mass enhancement was observed at a significantly higher rate in HER2 (+) cases. In addition, segmental distribution was prominent in all subtypes. Non-mass enhancement distribution and pattern were not found to differ significantly between subtypes, which is consistent with current publications. In similar studies, Navarro Vilar et al. (10) and Issar et al. (18) reported no significant difference in non-mass contrast enhancement distribution and patterns between molecular subtypes, as in our study.

We also investigated the accompanying focus in our study. None-of the molecular subtypes displayed focus presentation alone. However, the frequency of accompanying focus presentation was significantly higher in the luminal B subtype (p=0.008). Focus presentations are defined as morphological features that cannot be distinguished from ground contrast enhancement in terms of shape and margins because of insufficient contrast, often below 5 mm (19). However, the ACR BI-RADS Atlas provides limited data on focus presentation, and very few available studies have investigated the frequency of focus among molecular subtypes.

Our results also revealed significant differences between molecular subtypes in terms of axillary lymph node metastasis among BC cases (p=0.015). The most common subtype was luminal B in cases with positive axillary lymph nodes, which was attributed to the high number of luminal B cases. In fact, the highest prevalence belonged to HER2 (+) tumors at a rate of 66.7%, followed by luminal B at 55.7 (TN) BC at 43.1%, and luminal A at 39.8%. In addition, we observed axillary lymph node metastasis at a significantly higher rate in HER2 (+) tumors compared to HER2 (-) tumors ($p<0.05$). In their study, He et al. (20) reported axillary lymph node metastasis less frequently in (TN) BC cases than in other subtypes. In another study by Singh and Mukherjee (21), axillary lymph node metastasis was significantly higher in HR-\HER2+ cases, whereas HR +\HER2- cases exhibited significantly lower rates compared with other subtypes ($p<0.001$).

Study Limitations

Another study examining the difference between axillary lymph node metastasis and molecular subtypes yielded similar results to our study, reporting axillary lymph node metastasis at a significantly higher rate in triple-positive (HR+\HER2+) cases (22).

There are some limitations to our study. The single-center and retrospective design of our study was the main limitation. Unlike the BI-RADS atlas, the fact that the presentations were categorized as focus, mass alone, non-mass enhancement alone, and mass and non-mass enhancement alone groups may have caused the results to differ from the literature.

CONCLUSION

In conclusion, similar to our study, many available studies have reported morphological and physiological correlations between dynamic contrast-enhanced breast MRI findings and molecular subtypes (4-7). We believe that prospective studies with larger series should be conducted combining artificial intelligence with MRI so that MRI findings can better predict subtypes and prognostic factors.

Ethics

Ethics Committee Approval: Ethics committee approval was obtained for this study from the Ethics Committee of University of Health Sciences Turkey, Bakırköy Dr. Sadi Konuk Training and Research Hospital with decision number 2020 /538 and dated 21.12.2020.

Informed Consent: Obtained.

Peer-review: Externally peer-reviewed.

Authorship Contributions

Surgical and Medical Practices: N.E., A.A.G., E.İ., Concept: N.E., A.A.G., E.İ., Design: N.E., A.A.G., E.İ., Data Collection or Processing: N.E., A.A.G., E.İ., Analysis or Interpretation: N.E., Literature Search: N.E., Writing: N.E., A.A.G., E.İ.

Conflict of Interest: No conflict of interest was declared by the authors.

Financial Disclosure: The authors declared that this study received no financial support.

REFERENCES

1. Siegel RL, Miller KD, Jemal A. Cancer statistics, 2015. CA Cancer J Clin 2015;65:5-29.
2. Loo CE, Straver ME, Rodenhuis S, Muller SH, Wesseling J, Vrancken Peeters MJ, et al. Magnetic resonance imaging response monitoring of breast cancer during neoadjuvant chemotherapy: relevance of breast cancer subtype. J Clin Oncol 2011;29:660-6.
3. Bluemke DA, Gatsonis CA, Chen MH, DeAngelis GA, DeBruhl N, Harms S, et al. Magnetic resonance imaging of the breast prior to biopsy. JAMA 2004;292:2735-42.
4. Montemurro F, Martincich L, Sarotto I, Bertotto I, Ponzone R, Cellini L, et al. Relationship between DCE-MRI morphological and functional features and histopathological characteristics of breast cancer. Eur Radiol 2007;17:1490-7.
5. Tuncbilek N, Karakas HM, Okten OO. Dynamic magnetic resonance imaging in determining histopathological prognostic factors of invasive breast cancers. Eur J Radiol 2005;53:199-205.
6. Martincich L, Deantoni V, Bertotto I, Redana S, Kubatzki F, Sarotto I, Rossi V, Liotti M, Ponzone R, Aglietta M, Regge D, Montemurro F. Correlations between diffusion-weighted imaging and breast cancer biomarkers. Eur Radiol 2012;22:1519-28.
7. Chang YW, Kwon KH, Choi DL, Lee DW, Lee MH, Lee HK, et al. Magnetic resonance imaging of breast cancer and correlation with prognostic factors. Acta Radiol 2009;50:990-8.
8. Wilson DA, Kalisher L, Port JE, Titus JM, Kirzner HL. Breast imaging case of the day. Pure mucinous carcinoma with calcifying matrix. Radiographics 1997;17:800-4.
9. Ünçel M, Aköz G, Yıldırım Z, Pişkin G, Değirmenci M, Solakoğlu Kahraman D, et al. Evaluation Of Clinicopathological Features Of Breast Cancer According To The Molecular Subtypes. Journal of Tepecik Education and Research Hospital 2015;25:151–6.
10. Navarro Vilar L, Alandete Germán SP, Medina García R, Blanc García E, Camarasa Lillo N, Vilar Samper J. MR Imaging Findings in Molecular Subtypes of Breast Cancer According to BIRADS System. Breast J 2017;23:421-8.
11. Ab Mumin N, Ramli Hamid MT, Wong JHD, Rahmat K, Ng KH. Magnetic Resonance Imaging Phenotypes of Breast Cancer Molecular Subtypes: A Systematic Review. Acad Radiol 2022;29(Suppl 1):89-106.
12. Süha Öztürk V, Özgür R, Erdoğdu İH, Abacigil F, Taşkin F, Mrg M, et al. Can Breast MRI Findings Predict Molecular Subtypes of Breast Cancer? Akd Tıp D 2019;5:273–81.
13. Youk JH, Son EJ, Chung J, Kim JA, Kim EK. Triple-negative invasive breast cancer on dynamic contrast-enhanced and diffusion-weighted MR imaging: comparison with other breast cancer subtypes. Eur Radiol 2012;22:1724-34.
14. Algazzar MAA, Elsayed EEM, Alhanafy AM, Mousa WA. Breast cancer imaging features as a predictor of the hormonal receptor status, HER2neu expression and molecular subtype. Egyptian Journal of Radiology and Nuclear Medicine 2020;51:1–10.
15. Uematsu T, Kasami M, Yuen S. Triple-negative breast cancer: correlation between MR imaging and pathologic findings. Radiology 2009;250:638-47.
16. Kuhl C. The current status of breast MR imaging. Part I. Choice of technique, image interpretation, diagnostic accuracy, and transfer to clinical practice. Radiology 2007;244:356-78.
17. Kazama T, Takahara T, Hashimoto J. Breast Cancer Subtypes and Quantitative Magnetic Resonance Imaging: A Systemic Review. Life (Basel) 2022;12:490.
18. Issar P, Sinha S, Ravindranath M, Issar SK. MRI Features of Different Molecular subtypes of Breast Cancer. Indian Journal of Applied Radiology 2020;6:151-7
19. Carl J, D'Orsi EAS, Ellen B MEAMorris. ACR BI-RADS Atlas. Breast Imaging Reporting and Data System 5th Edition 2013. [Internet]. Carl J. D'Orsi EAS, Ellen B MEAMorris, editors. ACR BI-RADS Atlas. Breast Imaging Reporting and Data System 5th Edition 2013.
20. He ZY, Wu SG, Yang Q, Sun JY, Li FY, Lin Q, et al. Breast Cancer Subtype is Associated With Axillary Lymph Node Metastasis: A Retrospective Cohort Study. Medicine (Baltimore) 2015;94:e2213
21. Singh D, Mukherjee S. Impact of Molecular Subtypes of Breast Cancer on Axillary Lymph Node Metastasis: A Tertiary Center Experience. Archives of Breast Cancer 2021;8:305–12.
22. Em A. Ahmed ARH Ali A. Correlation of Breast Cancer Subtypes Based on ER, PR and HER2 Expression with Axillary Lymph Node Status. Cancer and Oncology Research 2014;2:51–7.